RSC Pharmaceutics

Accepted Manuscript

This article can be cited before page numbers have been issued, to do this please use: R. Siddiqui, M. Kawish, S. H. Khan, S. Habib, M. R. Shah, T. Shahrul Anuar, E. Brown and N. A. Khan, *RSC Pharm.*, 2025, DOI: 10.1039/D5PM00201J.

View Article Online
DOI: 10.1039/D5PM00201J

Effective targeting of pathogenic *Acanthamoeba castellanii* of the T4 genotype using nano-formulations of Quercetin

Ruqaiyyah Siddiqui[1,2#], Muhammad Kawish[3#], Simal Hassan Khan[1], Shahida Habib[3], Muhammad Raza Shah[3], Tengku Shahrul Anuar[4], Euan Brown[1], Naveed Ahmed Khan[5,2*]

[1]Institute of Biological Chemistry, Biophysics and Bioengineering, Heriot-Watt University Edinburgh, EH14 4AS UK; [2]Microbiota Research Center, Istinye University, Istanbul 34010, Turkey; [3]International Center for Chemical and Biological Sciences, H.E.J. Research Institute of Chemistry, University of Karachi, Karachi 75270, Pakistan; [4]Centre for Medical Laboratory Technology Studies, Faculty of Health Sciences, Universiti Teknologi MARA, Puncak Alam, Selangor, Malaysia; [5]School of Science, College of Science and Engineering, University of Derby, Derby, DE22 1GB, UK.

#Both authors contributed equally

Address for correspondence: N. A. Khan: School of Science, College of Science and Engineering, University of Derby, Derby, DE22 1GB, UK. E-mail: n.khan2@derby.ac.uk

View Article Online
DOI: 10.1039/D5PM00201J

Abstract

The incidence of infections caused by pathogenic *Acanthamoeba* is increasing, yet the prognosis continues to be poor. *Acanthamoeba* spp. are responsible for causing a blinding keratitis and a fatal granulomatous amoebic encephalitis. Due to limited options for the treatment of *Acanthamoeba* infections, there is a need for the development of effective drugs, which can target *Acanthamoeba* species. Zinc-copper nanoparticles show antimicrobial effects and enhance the effectiveness of their payload at specified biological targets. In this study, we used Quercetin and its' nanoconjugates and tested their anti-acanthamoebic properties. Quercetin was conjugated and loaded onto tragacanth polymer (a bioadhesive gum) coated with zinc copper bimetallic nanoparticles (QUE-TRG-ZnCuNPs) to enhance effects against *Acanthamoeba castellanii*. The characterization of the nanoconjugates was accomplished through fourier-transform infrared spectroscopy, ultraviolet visible spectrophotometry. Zeta potential, particle size, polydispersity index, scanning electron microscopy with energy-dispersive X-ray analysis were accomplished. Quercetin alone and its nanoconjugates were tested for the viability and growth of amoeba, encystation and excystation activity against *A. castellanii*, the cytopathogenicity assays were conducted to understand amoebae-mediated cytopathogenicity on host cells. The findings revealed that QUE-TRG-ZnCuNPs displayed significant anti-amoebic properties exhibiting up to 68% amoebicidal effects, up to 50% inhibition of encystation, and over 90% inhibition of excystmentagainst *A. castellanii*. Furthermore, QUE-TRG-ZnCuNPs reduced amoebae-mediated cytopathogenicity on host cells by up to 50%. These are promising findings and clearly suggest that Quercetin, combined with nanotechnology, could provide an effective strategy in the rationale development of therapeutics against *Acanthamoeba* infections.

Keywords: *Acanthamoeba castellanii;* Quercetin; Zn–Cu bimetallic nanoparticles*;* nanotechnology*;* keratitis; eye infection; free-living amoebae

View Article Online
DOI: 10.1039/D5PM00201J

Introduction

Acanthamoeba are free-living, eukaryotic, unicellular amoebae of significant relevance to human health, particularly as causative agents of granulomatous amoebic encephalitis (GAE), a severe central nervous system (CNS) infection, and *Acanthamoeba* keratitis (AK), a sight-threatening ocular infection (Visvesvara et al., 2007; Maciver et al., 2013; Walochnik, 2018; Rayamajhee et al., 2021; Henriquez et al., 2021).The prevalence of *Acanthamoeba* in the environment is widespread, with this pathogen being found in a variety of habitats, including soil, fresh water, and contaminated medical devices or contact lens cases (Kawaguchi et al., 2009; Bradbury et al., 2014; Bunsuwansakul et al., 2019 ;de Lacerda et al., 2021). Current treatment modalities for AK remain challenging, primarily due to the parasite's resilient cyst stage, which may lead to recurrence despite prolonged therapy (Lorenzo-Morales et al., 2015; Elsheikha et al., 2020; Kaufman and Tu, 2022; Campolo et al., 2022). Although biguanide and diamidine antimicrobial agents are commonly used, no single treatment is able to reliably eradicate AK (Alawfi et al., 2024).

In light of these challenges, nanotechnology has emerged as a promising approach for the development of novel therapeutic interventions. Quercetin (QUE), a flavonoid renowned for its antioxidant, anti-inflammatory, and antimicrobial properties, has demonstrated broad-spectrum efficacy against various pathogens (Nguyen et al., 2022). Its therapeutic potential is further amplified when conjugated with nanomaterials such as zinc oxide and/or copper, which may improve solubility, stability, and cellular uptake, thereby amplifying bioactivity (Salehi et al., 2020). Nanoconjugates can enhance antimicrobial efficacy through several mechanisms, including improved solubility and stability, enhanced cellular internalisation, and in some cases the generation of reactive oxygen species that contribute to pathogen killing. Zinc oxide and copper nanoparticles in particular have been shown to display stronger antimicrobial and antiparasitic effects than many other metals, owing to their ability to

View Article Online
DOI: 10.1039/D5PM00201J

disrupt cell membranes, induce oxidative stress, and interfere with enzymatic pathways (Sirelkhatim et al., 2015; El-Gebaly et al., 2024). These properties provided the rationale for selecting Zn–Cu nanoconjugates in the present study. Additionally, tragacanth, a natural gum with bio-adhesive and stabilising properties, is able to serve as a formidable carrier for enhancing the delivery and efficacy of bioactive compounds (Fahimirad, 2023). Quercetin has been widely studied for its antimicrobial and antiparasitic properties. For example, flavonoids have been reported to exert anti-parasitic activity against *Entamoeba histolytica* (Martínez-Castillo et al., 2018), and more recently quercetin conjugated with silver nanoparticles demonstrated significant effects on neuroinflammation, endothelial permeability, and pharmacokinetics against genotype T4 *Acanthamoeba polyphaga* (Abdel-Hakeem et al., 2025). These findings highlight Quercetin's potential as a therapeutic scaffold. Building on these observations, herein we explore the novel combination of quercetin with Zn–Cu bimetallic nanoparticles stabilized by tragacanth polymer. In this formulation, Quercetin-loaded, tragacanth polymer–coated Zn–Cu nanoparticles were prepared and their anti-amoebic effects investigated, presenting a distinctive approach to therapeutic development against *Acanthamoeba* trophozoites and cysts.

To this end, we performed a series of *in vitro* assays, including amoebicidal, amoebistatic, encystation and excystation analyses, cytotoxicity and cytopathogenicity analyses to assess the anti-amoebic properties of these conjugates. The amoebistatic assay was used to evaluate the ability of the conjugates to inhibit amoebic growth and proliferation, while the encystation and excystation assays were employed to assess their effects on the amoeba's ability to form cysts and transition back to the trophozoite form. Conjugation of Quercetin with zinc copper nanoparticles and tragacanth as a carrier/vector revealed potent amoebicidal activities, indicative of the potential of zinc-copper-quercetin-tragacanth conjugates as a novel therapeutic approach for *Acanthamoeba* infections.

View Article Online
DOI: 10.1039/D5PM00201J

Materials and methods

All solvents used in this study were HPLC-grade and purchased from Fisher Scientific, Copper (II) acetate monohydrate ($Cu(CH_3COO)_2.H_2O$), and Zinc acetate ($Zn(CH_3COO)_2.2H_2O$)), were obtained from Sigma-Aldrich, Merck Darmstadt, Germany. Tween 80 (T-80) was purchased from BDH, UK. The supplier of Tragacanth (TRG) was DAEJUNG (Korea) (MW: 20,000 daltons (average), degree of acetylation: ≤ 25%), and Quercetin (QUE) was purchased from Sigma Aldrich.

Preparation of Quercetin nanoconjugates

Tragacanth (TRG) stabilized bimetallic nanoparticles were synthesized in two steps. Firstly, (500 mg) was dissolved in water and placed on stirring for 3h at 50 ºC. The narrow-size, bimetallic nanoparticles (NPs) were synthesized by precipitating (10 mmol) Cu(II) and (20 mmol) Zn(II) in the above-prepared TRG solution solutions in an alkaline medium by a standard co-precipitation method, followed by the 2h stirring at 70 ºC. The prepared TRG-ZnCuNPs were washed thrice from D.I H_2O to remove unreacted salts and dried at high temperatures. A passive drug loading technique was used to prepare QUE-TRG-ZnCuNPs. In brief, TRG-ZnCuNPs (100 mg) were dispersed in D.I methanol and placed on stirring at room temperature. Then QUE (100 mg) was added carefully in suspension as mentioned earlier and allowed to progress under constant stirring for 24 h to facilitate the drug uptake. The QUE-TRG-ZnCuNPs were obtained via centrifugation at 12000 rpm and dried at room temperature.

Characterization and analysis

The average hydrodynamic diameter and polydispersity index (PDI) of drug-free (TRG-ZnCuNPs) and (QUE-TRG-ZnCuNPs) nanoparticles were investigated via using a Zetasizer (Zetasizer Nano ZS90 Malvern Instruments, Malvern, UK). Redispersed NPs were

View Article Online
DOI: 10.1039/D5PM00201J

transferred to a transparent plastic cuvette while being careful not to form bubbles. The Zetasizer evaluated the Zeta potential of freshly prepared formulations; diluted formulation was transferred to a cuvette dip-cell and added into the cuvette containing a solution, and the analysis was performed in triplicates. The cuvette was then inserted into the sample holder of the instrument, and analysis was conducted at 25 ºC. The medium viscosity, refractive index, and pressure were fixed at 1.0, 1.33, and 80.4 mPa, respectively. Nanoparticles were also characterized for their morphology using Scanning Electron Microscopy (Apreo 2C Lo Vac, USA). A drop of dispersed NPs samples was placed on aluminium stubs, air-dried at ambient temperature, and gold-sputtered before being scanned under the microscope.

FTIR Spectroscopy

Fourier Transformed Infrared (FTIR) Spectroscopy was conducted to assure the possible functionalization of substituents onto the surface of NPs and possible interaction in between drug and the NPs. In brief, about 1 mg of samples were mounted on an ATR assembly of the infrared spectrometer and the analysis were performed in between 4000-650 cm^{-1}.

Drug Entrapment Efficiency Determination (% DEE)

The drug entrapment efficiency of the developed QUE-TRG-ZnCuNPs was studied using a previously published protocol (Date et al., 2011; Katara et al., 2019). Concisely, the QUE loading nanoparticles were centrifuged at 12,000 rpm for 10 min to separate QUE-TRG-ZnCuNPs. The supernatant containing unbounded drug underwent successive dilutions and was then quantified at 360 nm on a UV-VIS spectrophotometer. The drug entrapment efficiencies were calculated by using the following relation:

$$\% \text{ Drug Entrapment} = \frac{\text{Total drug} - \text{unbound drug}}{\text{Total drug}} \times 100$$

View Article Online
DOI: 10.1039/D5PM00201J

In vitro Quercetin Release Profile

Using the dialysis method, an *in-vitro* QUE release study was carried out in different buffer solutions (pH 4.0 and 7.0) containing 0.1 % tween 80. About 5.0 mg QUE-TRG-ZnCuNPs were redispersed in deionized water (D.I H_2O 2ml) and then loaded into the dialysis bags (molecular weight cutoff of 12,000 kDa) with both ends fixed by clamps and immersed in a separate solution containing 30ml of phosphate saline buffer solutions (PBS) with a pH 4.0 or 7.0, followed by shaking at 150 rpm and 37 ^oC. At predetermined time intervals, 2ml aliquots were drawn and replaced with fresh buffer, and the QUE was quantified at 360 nm by UV visible spectrophotometer. Its amount was calculated using the standard calibration curve of QUE. All experiments were performed in triplicates using three different batches, and data were reported as mean values, and the standard deviations were calculated.

Cell Culture

Human Embryonic Kidney 293 (HEK293) cells were maintained in Dulbecco's Modified Eagle Medium (DMEM) supplemented with 10% foetal bovine serum (FBS) and 1% penicillin-streptomycin, as described previously (Mungroo et al., 2021). Cells were grown at 37°C in a humidified incubator with 5% CO_2. For routine sub-culture, cells were grown to 90% confluence. They were washed with phosphate-buffered saline (PBS) and detached using 0.05% trypsin-EDTA at 37°C for 10 minutes. Following trypsinisation the cells were centrifuged at 2000 rpm for 5 minutes. The pellet was resuspended in fresh medium and reseeded at the required density in 24 well plates for use in subsequent cytotoxicity and cytopathogenicity assays. All steps were performed aseptically in a laminar flow hood.

View Article Online
DOI: 10.1039/D5PM00201J

Cultivation of *Acanthamoeba castellanii* Trophozoites

Acanthamoeba castellanii (T4 genotype, ATCC 50492) were cultured in proteose peptone yeast glucose (PYG) medium containing 0.75% proteose peptone, 1.5% glucose, and 0.75% yeast extract. Cultures were maintained in axenic conditions at 30 °C, as previously described (Mungroo et al., 2021). The growth medium was refreshed every 20 hours to ensure active proliferation of trophozoites. Amoebae suspensions were monitored daily until a confluent layer of trophozoites was achieved, at which point the cells were harvested for experiments.

Preparation of *Acanthamoeba castellanii* cysts

To prepare cysts for subsequent assays, trophozoites were detached from culture flasks by chilling, collected, and centrifuged at 3000 × g for 10 minutes. Approximately 5×10^6 trophozoites were transferred onto non-nutritive agar plates to promote encystation through nutrient deprivation as described earlier (Mungroo et al., 2021). The plates were incubated at 30 °C for around two weeks, during which cyst formation was confirmed microscopically (Abjani et al., 2016). Subsequently, 10 mL of phosphate-buffered saline (PBS) was applied to the plates, and the cysts were scraped off using a cell scraper. Cysts were counted using a haemocytometer and used in subsequent assays.

Amoebicidal Analyses

To investigate the impact of Quercetin loaded tragacanth polymer coated zinc copper bimetallic nanoparticles (QUE-TRG-ZnCuNPs) on the viability of *Acanthamoeba castellanii* trophozoites, 5×10^5 amoebae per 0.5 mL per well were seeded in RPMI-1640 medium with 100 µg per mL of QUE-TRG-ZnCuNPs (Tragacanth polymer coated zinc copper bimetallic nanoparticles). QUE alone, Zn-Cu-TRG alone, chlorhexidine (anti-amoebic drug at 25 µg per mL) were utilised as controls. Other controls comprised amoeba alone or with corresponding solvent concentrations. The plates were incubated at 37 °C for 24 hours. Afterward, cidal

View Article Online
DOI: 10.1039/D5PM00201J

effects were assessed by adding 0.1% Trypan blue, and the number of living (unstained) and dead (stained) amoebae were counted using a haemocytometer.

Amoebistatic Analyses

Amoebistatic assays were conducted to assess the effects of quercetin loaded tragacanth polymer coated zinc copper bimetallic nanoparticles on the growth of *A. castellanii* (Mungroo et al., 2021). Trophozoites (5×10^5) were incubated with 100 µg per mL of QUE-TRG-ZnCuNPs, Zn-Cu-TRG, QUE in PYG growth medium in 24-well plates. The plates were maintained at 30 °C for 48 hours. Control conditions included trophozoites in 100% PYG, non-nutritive phosphate-buffered saline (PBS), and solvent-containing PYG, as well as Zn-Cu-TRG, QUE, and chlorhexidine (25 µg per mL). The number of amoebae was then quantified using a haemocytometer.

Encystation Analyses

To assess the influence of quercetin loaded tragacanth polymer coated zinc copper bimetallic nanoparticles QUE-TRG-ZnCuNPs on cyst formation at 100 µg per mL, encystation was triggered by inoculating 2×10^6 amoebae in PBS containing 50 mM $MgCl_2$ and 10% glucose in a 24-well plate, which was incubated at 30 °C for 72 hours without shaking (Mungroo et al., 2021). After incubation, SDS (0.5%) was added for 10 minutes to solubilize trophozoites, and the cysts were counted using a haemocytometer. Control wells contained QUE alone, Zn-Cu-TRG alone, chlorhexidine (anti-amoebic drug at 25 µg per mL), and negative controls lacked both compounds and the encystation trigger. Solvent controls were included with amoebae and compounds. Cysts were counted using a haemocytometer (Mungroo et al., 2021).

Excystation Analyses

To investigate if quercetin loaded tragacanth polymer coated zinc copper bimetallic nanoparticles QUE-TRG-ZnCuNPs hinder the transition of amoebae from the dormant cyst

View Article Online
DOI: 10.1039/D5PM00201J

stage to the active trophozoite stage, excystation tests were conducted as outlined in previous studies (Mungroo et al., 2021). In the excystation assays, an initial inoculum of approximately 5×10^5 mature cysts per well, harvested after 10–12 days of encystation on non-nutrient agar plates as described above. Following this, the cysts were incubated with quercetin loaded tragacanth polymer coated zinc copper bimetallic nanoparticles QUE-TRG-ZnCuNPs at 100 µg per mL in PYG growth medium to assess whether the treatments could prevent the transformation of cysts into active trophozoites. The cysts were incubated in the growth medium for up to 72 hours. Controls as described above were utilised, as well as amoebae alone and were assessed by counting the trophozoites that excysted using a haemocytometer.

Cytotoxicity Assays using Lactate dehydrogenase (LDH)

Cytotoxicity assays were conducted using HEK293 cells as previously described (Mungroo et al., 2021). Once fully confluent monolayers of HEK293 cells were established, the medium was replaced with fresh serum-free medium, with 100 µg per mL of QUE-TRG-ZnCuNPs and control compounds, and solvent controls described above were added to 24-well plates. The plates were incubated in a humidified atmosphere with 5% CO_2 at 37 °C for 24 hours. After this incubation, 0.1% Triton X-100 detergent was added as a positive control for 100% cell death, while untreated HEK293 cells served as the negative control. Supernatants were collected from the wells, and the lactate dehydrogenase (LDH) cytotoxicity detection kit (Roche) was used to assess LDH release, following the manufacturer's instructions to determine the percentage of cell death or cytotoxicity. Cytotoxicity percentage was calculated using the following formula: (sample absorbance – negative control absorbance) / (positive control absorbance – negative control absorbance) × 100%.

View Article Online
DOI: 10.1039/D5PM00201J

In vitro cytopathogenicity Analyses

To assess whether quercetin loaded tragacanth polymer coated zinc copper bimetallic nanoparticles QUE-TRG-ZnCuNPs at 100 µg per mL can prevent parasite-induced damage to host cells, *in vitro* cytopathogenicity tests were performed as previously described (Mungroo et al., 2021). In brief, *A. castellanii* (5×10^5 amoebae) were exposed to quercetin loaded tragacanth polymer coated zinc copper bimetallic nanoparticles QUE-TRG-ZnCuNPs at 100 µg per mL and controls (as described above) for 2 hours at 30 °C. After treatment, the amoebae were centrifuged at 1500× g for 2 minutes, and the pellet was resuspended in 200 µL of RPMI-1640. These amoebae were then introduced onto HEK293 cells grown in 96-well plates and incubated for 24 hours. Host cell damage was then evaluated using LDH assays, as described earlier above.

Statistical Analyses

Statistical significance was determined using a two-sample t-test with a two-tailed distribution. P-values < 0.05 were considered statistically significant. The graphical data display standard errors on the y-axis.

Results

Successful preparation of Quercetin nanoconjugates (TRG-ZnCuNPs and QUE-TRG-ZnCuNPs)

FTIR spectra of TRG showed prominent peaks of OH (Stretching), C-H (Stretching), and C-O-C (Stretching) at 3382 cm^{-1}, 2984 cm^{-1}, and 1038 cm^{-1} as presented in Figure 1 (Ihsan et al., 2024). The absorption frequencies of TRG shifted slightly when it was modified onto the surface of ZnCuNPs. For Instance, the peak of OH was moved from 3382 to 3370 cm^{-1} (Figure 1). The peak of C=O was shifted from 1670 to 1650 cm^{-1}, and C-O-C was shifted from 1038 to 1023 cm^{-1}, implying that these functional groups were involved in

View Article Online
DOI: 10.1039/D5PM00201J

chelation with the surface of ZnCuNPs. As depicted in (Figure 2) the Quercetin (QUE) molecule revealed a characteristic absorption at 3250 m^{-1}, 1660 cm^{-1}, and 1043 cm^{-1} corresponding to OH stretching, C=O and C-O, respectively (Kawish et al., 2024). In FTIR spectra of QUE-TRG-ZnCuNPs (Figure 3), these bands were shifted slightly, 3238 cm^{-1}, 1631 cm^{-1}, and 1037 cm^{-1}, indicating that OH, C=O and C-O-C groups of QUE were involved in chelation with TRG-ZnCuNPs. The slight variation in FTIR values also suggested that secondary interaction was responsible for the entrapment of QUE onto the surface of TRG-ZnCuNPs.

Particle size, polydispersity index, zeta potential, and scanning electron microscopy with energy-dispersive X-ray analysis.

Dynamic light scattering analysis showed that the average diameter of QUE-TRG-ZnCuNPs was greater than unbounded TRG-ZnCuNPs, as depicted in (Table 1). The increment in size may be due to the association of QUE with the surface of TRG-ZnCuNPs (Kawish et al., 2021). Due to the abundance of the COO- group on the TRG skeleton, the functionalized TRG-ZnCuNPs showed negative zeta potential values (Table 1), but when QUE was loaded onto TRG-ZnCuNPs, the zeta potential values were changed to more negative, indicating that COO^- was more exposed onto the surface of QUE-CHI-ZnCuNPs (Kawish et al., 2021). Moreover, particle aggregation is less likely to occur in nanomaterials with high zeta potential values because it raises columbic repulsions and increases colloidal stability (Kawish et al., 2021). Polydispersity index (PDI) values show the colloidal stability of nanoparticles and values less than 0.5 indicate colloidal uniformity. The PDI values in the case of our designed QUE-TRG-ZnCuNPs are less than 0.5, representing that the nanoformulation is colloidally stable.

View Article Online
DOI: 10.1039/D5PM00201J

Scanning electron microscopic images revealed that the developed TRG-ZnCuNPs and QUE-TRG-ZnCuNPs were nearly spherical in morphology, as represented in (Figure 3). As expected, energy-dispersive X-ray analysis revealed a vast difference in the elemental composition of developed TRG-ZnCuNPs and QUE-TRG-ZnCuNPs. In the case of TRG-ZnCuNPs, the elemental composition of C (63.4 %), O (29.2 %), Zn (4.7 %), and Cu (2.3 %) was observed (Figure 3A). Furthermore, in the case of QUE-TRG-ZnCuNPs, the composition varied to C (71.0 %), O (20.6 %), Zn (6.7 %), and Cu (1.7 %) (Figure 3B), which may be due to the entrapment of QUE onto the surface of TRG-ZnCuNPs.

Drug Entrapment Efficiency Determination

Herein, the passive drug-loading technique was adopted because QUE belongs to the class of polyphenols, and the method facilitates the chelation of phenolic and other moieties with the metal cores [7]. The drug's entrapment efficiency of QUE within QUE-TRG-ZnCuNPs was found to be 58.6 ±2.85%. The increased QUE loading was attributed to enhanced hydrogen bonding between QUE and the conjugated TRG moiety.

***In-Vitro* QUE Release**

The release patterns of QUE were analysed in two different media, pH 7.0 and pH 4.0, which are indicative of a physiological and infectious microenvironment, respectively. According to the drug release plots (Figure 4), at pH 7.0, the onset of drug release was relatively faster than at pH 4.0. The cumulative release of QUE from QUE-TRG-ZnCuNPs within 24 h at pH 7.0 and 4.0 was about 72 ±1.36 % and 45.3 ±0.78 % respectively. The higher drug release at neutral pH may be due to the enhancement of columbic repulsions between QUE and TRG-ZnCuNPs, which triggers the QUE release.

View Article Online
DOI: 10.1039/D5PM00201J

Quercetin loaded tragacanth polymer coated zinc copper bimetallic nanoparticles reveal significant amoebicidal properties against *A. castellanii*

Amoebicidal experimentation yielded the anti-amoebic efficacy caused by QUE-TRG-ZnCuNPs against *A. castellanii.* Following incubation of the amoeba with 100µg/mL of the compounds, significant (T-test, two-tail distribution, P≤0.05) amoebicidal activity was reported in QUE-TRG-ZnCuNPs and Quercetin alone reducing amoeba viability to approximately 50% as depicted in Figure 5. Of note, the anti-amoebic drug chlorhexidine revealed more than 90% amoebicidal effects, whereas the solvent control of DMSO showed no apparent cidal effects. Furthermore, QUE alone, Zn-Cu-TRG alone revealed limited effects as depicted in Figure 5.

Quercetin loaded tragacanth polymer coated zinc copper bimetallic nanoparticles reveal significant amoebistatic properties against *A. castellanii*

Amoebistatic experimentation yielded the effects caused by QUE-TRG-ZnCuNPs against the growth of *A. castellanii.* Following incubation of the amoeba with 100µg/mL of the compounds, significant (T-test, two-tail distribution, P≤0.05) amoebistatic activity was reported in QUE-TRG-ZnCuNPs and Quercetin alone reducing amoeba growth to approximately 50% compared to amoeba alone, as depicted in Figure 6. Of note, the anti-amoebic drug chlorhexidine revealed more than 90% amoebistatic effects, whereas the solvent control of DMSO showed limited or no apparent static effects, revealing more than 90% amoebae growth as compared to amoebae alone. Furthermore, Zn-Cu-TRG alone also revealed limited static effects, instead showing amoebae growth at more than 90%, whereas QUE alone had some effects, although these were not significant, as depicted in Figure 6.

View Article Online
DOI: 10.1039/D5PM00201J

Quercetin loaded tragacanth polymer coated zinc copper bimetallic nanoparticles significantly reduced encystment of *A. castellanii*

Encystation analyses revealed the effects caused by QUE-TRG-ZnCuNPs against the ability of amoebae to differentiate into cysts. Following incubation of the amoeba with 100µg/mL of the compounds, significant (T-test, two-tail distribution, P≤0.05) encystation effects were revealed in QUE-TRG-ZnCuNPs and QUE, which both revealed significant effects on encystation, approximately 50% and 56% in comparison to 100% encystment or encystment media as shown in Figure 7. Of note, the anti-amoebic drug chlorhexidine revealed more than 90% effects on encystation, whereas the solvent control of DMSO showed limited or no apparent effects, Furthermore, Zn-Cu-TRG alone also revealed limited effects on encystation.

Quercetin loaded tragacanth polymer coated zinc copper bimetallic nanoparticles reveal significant effects on the excystment of *A. castellanii*

Analyses of excystation assays revealed the effects caused by QUE-TRG-ZnCuNPs against the ability of cysts to transform back to the trophozoite stage. Following incubation of the cysts with 100µg/mL of the compounds, and addition of PYG growth media significant (T-test, two-tail distribution, P≤0.05) excystment effects were revealed in QUE-TRG-ZnCuNPs and QUE, which both revealed significant effects on excystation, of around 90% inhibition of excystment in comparison to amoeba alone, as shown in Figure 8. Of note, the anti-amoebic drug chlorhexidine revealed more than 95% effects on excystation, whereas the solvent control of DMSO showed limited or no apparent effects, Furthermore, Zn-Cu-TRG alone also revealed limited effects on excystation of around 30% and Quercetin of around 67% excystment inhibition (Figure 8).

View Article Online
DOI: 10.1039/D5PM00201J

Quercetin loaded tragacanth polymer coated zinc copper bimetallic nanoparticles reduced *A. castellanii* cytopathogenicity

Assays were performed to evaluate if Quercetin loaded tragacanth polymer coated zinc copper bimetallic nanoparticles can inhibit amoebae-mediated host cell damage. When compared with the negative control, quercetin loaded tragacanth polymer coated zinc copper bimetallic nanoparticles, reduced amoebae-driven human cell cytopathogenicity. Overall, human cell damage was reduced 55% in human cells treated with amoeba alone and 26.6% in cells pre-incubated with quercetin loaded tragacanth polymer coated zinc copper bimetallic nanoparticles within 24h, revealing a significant reduction in amoeba-mediated cell cytopathogenicity, as shown in Figure 9. In contrast, Zn-Cu-TRG and QUE did not significantly affect amoebae-mediated host cell death.

Discussion

Acanthamoeba spp. are ubiquitous free-living amoebae found in diverse environments, including soil, freshwater, and air-conditioning systems (Schuster and Visvesvara, 2004; Bullé et al., 2020; Chaúque et al., 2022). They can cause severe human infections, most notably *Acanthamoeba keratitis* (AK), a painful and sight-threatening corneal infection primarily affecting contact lens users (Carnt and Stapleton, 2016; Niederkorn, 2021). AK cases have been rising globally, with conventional treatment relying on biguanides and diamidines, which require prolonged use and may cause corneal toxicity (Zhang et al., 2023). Of note, in the UK, the incidence of AK has been notably high, particularly in Scotland, where the west region reports around 7.0 cases per million people (Illingworth et al., 1995; Seal et al., 1999; Zhang et al., 2023). The rise in AK cases in the UK is believed to be linked to the increased use of contact lenses since 1992 (Illingworth et al., 1995; Zhang et al., 2023). Additionally, *Acanthamoeba*'s ability to form resilient cysts makes treatment even more challenging, often leading to recurrence and treatment failure (Abjani et

View Article Online
DOI:10.1039/D5PM00201J

al., 2016). These challenges highlight the urgent need for novel, more effective therapeutic strategies. Given that previous studies have shown Quercetin and ZnO to possess significant anti-amoebic effects against *Balamuthia mandrillaris* and *Naegleria fowleri* (Siddiqui et al., 2022) and considering the current lack of effective treatments for *Acanthamoeba castellanii* infections, this provided the rationale for investigating their potential against *Acanthamoeba* in the present study. Thus, a novel formulation was developed by incorporating Quercetin-loaded tragacanth polymer-coated zinc-copper bimetallic nanoparticles, and its anti-amoebic effects were evaluated.

The successful synthesis and characterisation of Quercetin-loaded tragacanth polymer-coated zinc-copper bimetallic nanoparticles (QUE-TRG-ZnCuNPs) demonstrated their colloidal stability, uniformity, and efficient drug entrapment. The increase in particle size and zeta potential upon Quercetin loading suggested strong interactions between the polymeric TRG-ZnCuNPs and Quercetin molecules, enhancing drug entrapment efficiency (58.6%). *In vitro* drug release studies showed pH-dependent behaviour, with faster Quercetin release at physiological pH (7.0) than in acidic conditions (pH 4.0), likely due to increased electrostatic repulsions.

Functionally, QUE-TRG-ZnCuNPs exhibited significant anti-amoebic activity against *Acanthamoeba castellanii*, reducing trophozoite viability, growth, and encystation while also inhibiting excystation and amoeba-mediated human cell cytopathogenicity. Notably, QUE-TRG-ZnCuNPs were more effective than Quercetin alone, likely due to enhanced bioavailability and sustained release. Furthermore, zinc and copper nanoparticles, as well as tragacanth alone, were included as controls, in line with our practice of evaluating individual components alongside the conjugates. Consistent with this, our previous work has demonstrated that metallic nanoparticles formulated with natural gums or flavonoids exhibit anti-amoebic activity against *Acanthamoeba castellanii* (Anwar et al., 2019). In the current

View Article Online
DOI: 10.1039/D5PM00201J

assays, zinc and copper nanoparticles alone produced moderate inhibition of trophozoite viability and partial effects on cyst stages, while tragacanth alone showed negligible anti-amoebic activity, as in our previous work (Anwar et al., 2019). By contrast, the Quercetin–Zn–Cu–tragacanth conjugates demonstrated markedly higher amoebicidal and cysticidal efficacy, suggesting the synergistic contribution of the combined components. These findings reinforce the rationale for integrating Quercetin with Zn–Cu nanoparticles and tragacanth in a single formulation for enhanced anti-amoebic activity.

Of note, while the nanoconjugates in our study showed promising amoebicidal and amoebistatic effects, their efficacy remained lower than that of chlorhexidine, an anti-amoebic agent. Although chlorhexidine demonstrated stronger anti-amoebic activity in our assays, its well-documented ocular cytotoxicity and limited tolerability remain major drawbacks for clinical use (Fernández-Ferreiro et al., 2017. Shigeyasu et al., 2012). Current therapeutic regimens, including biguanides and diamidines, are often prolonged, associated with poor patient compliance, and do not always reliably eradicate infection. In this context, nanoformulations such as QUE-TRG-ZnCuNPs may provide important advantages, including reduced cytotoxicity, sustained drug release, improved physicochemical stability, and the potential for ocular bio-adhesion through the tragacanth polymer. These features suggest that QUE-TRG-ZnCuNPs could represent a safer and more biocompatible alternative for the long-term management of *Acanthamoeba* infections.

The precise mechanism of action of these compounds against *Acanthamoeba* remains unclear. However, zinc oxide nanoparticles are known to exhibit antimicrobial activity by disrupting cell wall integrity and altering membrane permeability, primarily through the generation of reactive oxygen species (Sirelkhatim et al., 2015). In a study on *Campylobacter jejuni*, ZnO nanoparticles were found to interact with bacterial cell surfaces either directly or via electrostatic interactions, potentially leading to cellular internalisation and oxidative stress

View Article Online
DOI: 10.1039/D5PM00201J

through reactive oxygen species production (Xie et al., 2011). Additionally, these compounds may induce apoptosis within *Acanthamoeba*, as ZnO nanoparticles have previously been shown to trigger apoptosis in human cancer cells (Wahab et al., 2014).

Analogous studies have reported that metallic nanoparticles such as ZnO induce oxidative stress, membrane damage, and apoptosis-like changes in protozoan parasites. For example, ZnO nanoparticles caused oxidative damage and morphological alterations in *Leishmania major* (Delavari et al., 2014), while gold–silver bimetallic nanoparticles induced ROS-mediated apoptosis-like death in *Leishmania donovani* promastigote and amastigote stages (Alti et al., 2020). Our own previous work has also demonstrated that QUE conjugated with silver nanoparticles (QUE-AgNPs) displays enhanced anti-amoebic activity against *A. castellanii* relative to QUE or AgNPs alone (Anwar et al., 2020). Although the present study did not measure ROS, apoptosis markers, or ultrastructural changes in *Acanthamoeba*, these findings support the hypothesis that similar mechanisms may underlie the enhanced efficacy of the QUE-TRG-ZnCuNPs formulation.

Given the bioadhesive properties of tragacanth gum (Boamah et al., 2023), this formulation could be suitable for topical ophthalmic application, particularly for AK. The sustained and pH-dependent drug release facilitated by tragacanth may enhance ocular retention and prolong residence time on the corneal surface, thereby improving treatment efficacy. Additionally, the antimicrobial activity of Zn–Cu nanoparticles and QUE could help target both trophozoites and cysts, addressing one of the major challenges in AK treatment. Further studies are required to assess the formulation's stability, biocompatibility, and *in vivo* efficacy to establish its potential as a viable therapeutic option. These findings indicate that QUE-TRG-ZnCuNPs could serve as a potential therapeutic intervention against *A. castellanii*, warranting further investigation into their mechanism of action and *in vivo* efficacy.

View Article Online
DOI: 10.1039/D5PM00201J

Conclusion

In conclusion, quercetin-loaded tragacanth polymer-coated zinc-copper bimetallic nanoparticles (QUE-TRG-ZnCuNPs) were successfully developed and tested for their anti-amoebic effects against *Acanthamoeba castellanii*. The results demonstrated significant amoebicidal, amoebistatic, encystment and excystment inhibiting activities, with QUE-TRG-ZnCuNPs effectively reducing the viability, growth, encystment, and excystment of the amoeba. The compounds showed reduced amoebae-mediated cytopathogenicity effects on human cells, highlighting their potential therapeutic application. Future studies will focus on further elucidating the mechanism of action. *In vivo* studies will also be essential to confirm the safety and efficacy of QUE-TRG-ZnCuNPs in a biological context. Additionally, the potential application of these nanoconjugates in water treatment and other related fields should be explored.

Ethical Approval: Not applicable.

Competing interests: Not applicable.

Authors contributions: RS, and NAK conceptualized the study amid discussions with MRS. MK, and SH carried out all experiments related to chemistry under the supervision of MRS. All microbiology-related experiments were carried out by SHK, and TSA under the supervision of RS, EB and NAK. MK, SH, and SHK analysed the data. MK, RS, and NAK prepared the first draft of the manuscript. NAK corrected the manuscript. All authors agreed with the final manuscript.

Funding: Ruqaiyyah Siddiqui and Naveed Ahmed Khan are supported by the Air Force Office of Scientific Research (AFOSR).

Availability of data and materials: The data supporting this article have been included in the manuscript.

References

1. Abdel-Hakeem SS, Abdel-Samiee MAZ, Khalaf MMA, Abed GH. Impact of quercetin conjugated silver nanoparticles on neuroinflammation, endothelial permeability, and pharmacokinetics in vivo against genotype T4, Acanthamoeba polyphaga. J Drug Deliv Sci Technol. 2025;107116.
2. Abjani F, Khan NA, Yousuf FA, Siddiqui R. Targeting cyst wall is an effective strategy in improving the efficacy of marketed contact lens disinfecting solutions against Acanthamoeba castellanii cysts. Contact Lens Anterior Eye. 2016;39(3):239-43.
3. Alawfi BS, Khan NA, Lloyd D, Siddiqui R. Acanthamoeba keratitis: new hopes for potential interventions for a curable but often refractory disease. Expert Rev Ophthalmol. 2024;19(4):71-80.
4. Alti D, Veeramohan Rao M, Rao DN, Maurya R, Kalangi SK. Gold–silver bimetallic nanoparticles reduced with herbal leaf extracts induce ROS-mediated death in both promastigote and amastigote stages of Leishmania donovani. ACS Omega. 2020;5(26):16238-45.
5. Anwar A, Masri A, Rao K, Rajendran K, Khan NA, Shah MR, Siddiqui R. Antimicrobial activities of green synthesized gums-stabilized nanoparticles loaded with flavonoids. Sci Rep. 2019;9(1):3122.
6. Boamah PO, Afoakwah NA, Onumah J, Osei ED, Mahunu GK. Physicochemical properties, biological properties and applications of gum tragacanth – a review. Carbohydr Polym Technol Appl. 2023;5:100288.
7. Bradbury RS, French LP, Blizzard L. Prevalence of Acanthamoeba spp. in Tasmanian intensive care clinical specimens. J Hosp Infect. 2014;86(3):178-81.
8. Bullé DJ, Benittez LB, Rott MB. Occurrence of Acanthamoeba in hospitals: a literature review. Rev Epidemiol Controle Infec. 2020;10(2):174-80.
9. Bunsuwansakul C, Mahboob T, Hounkong K, Laohaprapanon S, Chitapornpan S, Jawjit S, Yasiri A, Barusrux S, Bunluepuech K, Sawangjaroen N, Salibay CC. Acanthamoeba in Southeast Asia: overview and challenges. Korean J Parasitol. 2019;57(4):341.
10. Campolo A, Pifer R, Walters R, Thomas M, Miller E, Harris V, King J, Rice CA, Shannon P, Patterson B, Crary M. Acanthamoeba spp. aggregate and encyst on contact lens material increasing resistance to disinfection. Front Microbiol. 2022;13:1089092.
11. Carnt N, Stapleton F. Strategies for the prevention of contact lens-related Acanthamoeba keratitis: a review. Ophthalmic Physiol Opt. 2016;36(2):77-92.
12. Chaúque BJM, Dos Santos DL, Anvari D, Rott MB. Prevalence of free-living amoebae in swimming pools and recreational waters: a systematic review and meta-analysis. Parasitol Res. 2022;121(11):3033-50.
13. Date AA, Nagarsenker MS, Patere S, Dhawan V, Gude RP, Hassan PA, Aswal V, Steiniger F, Thamm J, Fahr A. Lecithin-based novel cationic nanocarriers (Leciplex)

DOI: 10.1039/D5PM00201J

II: improving therapeutic efficacy of quercetin on oral administration. Mol Pharm. 2011;8(3):716-26.
14. de Lacerda AG, Lira M. Acanthamoeba keratitis: a review of biology, pathophysiology and epidemiology. Ophthalmic Physiol Opt. 2021;41(1):116-35.
15. Delavari M, Dalimi A, Ghaffarifar F, Sadraei J. In vitro study on cytotoxic effects of ZnO nanoparticles on promastigote and amastigote forms of Leishmania major (MRHO/IR/75/ER). Iran J Parasitol. 2014;9(1):6.
16. El-Gebaly AS, Sofy AR, Hmed AA, Youssef AM. Green synthesis, characterization and medicinal uses of silver nanoparticles (Ag-NPs), copper nanoparticles (Cu-NPs) and zinc oxide nanoparticles (ZnO-NPs) and their mechanism of action: a review. Biocatal Agric Biotechnol. 2024;55:103006.
17. Elsheikha HM, Siddiqui R, Khan NA. Drug discovery against Acanthamoeba infections: present knowledge and unmet needs. Pathogens. 2020;9(5):405.
18. Fahimirad S. Gum tragacanth-based nanosystems for therapeutic applications. In: Polymeric Nanosystems. Cambridge (MA): Academic Press; 2023. p. 367-404.
19. Fernández-Ferreiro A, Santiago-Varela M, Gil-Martinez M, González-Barcia M, Luaces-Rodriguez A, Diaz-Tome V, Pardo M, Méndez JB, Pineiro-Ces A, Rodríguez-Ares MT, Lamas MJ. In vitro evaluation of the ophthalmic toxicity profile of chlorhexidine and propamidine isethionate eye drops. J Ocul Pharmacol Ther. 2017;33(3):202-9.
20. Henriquez FL, Mooney R, Bandel T, Giammarini E, Zeroual M, Fiori PL, Margarita V, Rappelli P, Dessì D. Paradigms of protist/bacteria symbioses affecting human health: Acanthamoeba species and Trichomonas vaginalis. Front Microbiol. 2021;11:616213.
21. Ihsan S, Munir H, Meng Z, Tayyab M, Zeeshan N, Rehman A, Nadeem S, Irfan M. Tragacanth gum-based copper oxide nanoparticles: comprehensive characterization, antibiofilm, antimicrobial and photocatalytic potentials. Int J Biol Macromol. 2024;268:131600.
22. Illingworth CD, Cook SD, Karabatsas CH, Easty D. Acanthamoeba keratitis: risk factors and outcome. Br J Ophthalmol. 1995;79(12):1078-82.
23. Kaufman AR, Tu EY. Advances in the management of Acanthamoeba keratitis: a review of the literature and synthesized algorithmic approach. Ocul Surf. 2022;25:26-36.
24. Katara R, Sachdeva S, Majumdar DK. Design, characterization, and evaluation of aceclofenac-loaded Eudragit RS 100 nanoparticulate system for ocular delivery. Pharm Dev Technol. 2019;24(3):368-79.
25. Kawaguchi K, Matsuo J, Osaki T, Kamiya S, Yamaguchi H. Prevalence of Helicobacter and Acanthamoeba in natural environment. Lett Appl Microbiol. 2009;48(4):465-71.
26. Kawish M, Jabri T, Elhissi A, Zahid H, Muhammad Iqbal K, Rao K, Gul J, Abdullah M, Shah MR. Galactosylated iron oxide nanoparticles for enhancing oral bioavailability of ceftriaxone. Pharm Dev Technol. 2021;26(3):291-301.

27. Kawish M, Parveen S, Siddiqui NN, Jahan H, Elhissi A, Yasmeen S, Raza Shah M. Highly functionalized pH-triggered supramolecular nanovalve for targeted cancer chemotherapy. Pharm Dev Technol. 2024;29(7):751-61.
28. Lorenzo-Morales J, Khan NA, Walochnik J. An update on Acanthamoeba keratitis: diagnosis, pathogenesis and treatment. Parasite. 2015;22:10.1051/parasite/2015022.
29. Maciver SK, Asif M, Simmen MW, Lorenzo-Morales J. A systematic analysis of Acanthamoeba genotype frequency correlated with source and pathogenicity: T4 is confirmed as a pathogen-rich genotype. Eur J Protistol. 2013;49(2):217-21.
30. Martínez-Castillo M, Pacheco-Yepez J, Flores-Huerta N, Guzmán-Téllez P, Jarillo-Luna RA, Cárdenas-Jaramillo LM, Campos-Rodríguez R, Shibayama M. Flavonoids as a natural treatment against Entamoeba histolytica. Front Cell Infect Microbiol. 2018;8:209.
31. Mungroo MR, Tong T, Khan NA, Anuar TS, Maciver SK, Siddiqui R. Development of anti-acanthamoebic approaches. Int Microbiol. 2021;24:363-71.
32. Niederkorn JY. The biology of Acanthamoeba keratitis. Exp Eye Res. 2021;202:108365.
33. Nguyen TLA, Bhattacharya D. Antimicrobial activity of quercetin: an approach to its mechanistic principle. Molecules. 2022;27(8):2494.
34. Rayamajhee B, Subedi D, Peguda HK, Willcox MD, Henriquez FL, Carnt N. A systematic review of intracellular microorganisms within Acanthamoeba to understand potential impact for infection. Pathogens. 2021;10(2):225.
35. Salehi B, Machin L, Monzote L, Sharifi-Rad J, Ezzat SM, Salem MA, Merghany RM, El Mahdy NM, Kılıç CS, Sytar O, Sharifi-Rad M. Therapeutic potential of quercetin: new insights and perspectives for human health. ACS Omega. 2020;5(20):11849-72.
36. Schuster FL, Visvesvara GS. Free-living amoebae as opportunistic and non-opportunistic pathogens of humans and animals. Int J Parasitol. 2004;34(9):1001-27.
37. Seal DV, Kirkness CM, Bennett HGB, Peterson M, Keratitis Study Group. Population-based cohort study of microbial keratitis in Scotland: incidence and features. Contact Lens Anterior Eye. 1999;22(2):49-57.
38. Shigeyasu C, Shimazaki J. Ocular surface reconstruction after exposure to high concentrations of antiseptic solutions. Cornea. 2012;31(1):59-65.
39. Siddiqui R, Boghossian A, Akbar N, Jabri T, Aslam Z, Shah MR, Alharbi AM, Alfahemi H, Khan NA. Zinc oxide nanoconjugates against brain-eating amoebae. Antibiotics. 2022;11(10):1281.
40. Sirelkhatim A, Mahmud S, Seeni A, Kaus NHM, Ann LC, Bakhori SKM, Hasan H, Mohamad D. Review on zinc oxide nanoparticles: antibacterial activity and toxicity mechanism. Nano-Micro Lett. 2015;7(3):219-42.
41. Visvesvara GS, Moura H, Schuster FL. Pathogenic and opportunistic free-living amoebae: Acanthamoeba spp., Balamuthia mandrillaris, Naegleria fowleri, and Sappinia diploidea. FEMS Immunol Med Microbiol. 2007;50(1):1-26.
42. Walochnik J. Amoebae. In: Parasitic Protozoa of Farm Animals and Pets. Cham: Springer; 2018. p. 389-412.

43. Zhang Y, Xu X, Wei Z, Cao K, Zhang Z, Liang Q. The global epidemiology and clinical diagnosis of Acanthamoeba keratitis. J Infect Public Health. 2023;16(6):841-52.

View Article Online
DOI: 10.1039/D5PM00201J

List of Figures

Figure 1: FTIR spectra of TRG and TRG-ZnCuNPs.

Figure 2: FTIR spectra of QUE and QUE-TRG-ZnCuNPs.

Figure 3: SEM analysis of (A) TRG-ZnCuNPs: (i) SEM image, (ii) EDX image, (iii) EDX spectrum, (iv) EDX image with elemental mapping, (B) QUE-TRG-ZnCuNPs: (i) SEM image, (ii) EDX image, (iii) EDX spectrum, (iv) EDX image with elemental mapping.

Figure 4: In vitro drug release profiles at pH 7.0 and 4.0.

Figure 5: Quercetin loaded tragacanth polymer coated zinc copper bimetallic nanoparticles reveal significant amoebicidal properties against *A. castellanii*

(a) At 100 µg per mL, QUE-TRG-ZnCuNPs and Quercetin alone demonstrated significant amoebicidal activity, significantly reducing amoeba viability after 24 hours of incubation. The data is representative of at least 3 independent experiments, performed in duplicate, and are presented as the mean ± standard error. Additionally, P-values were calculated using a two-sample t-test with a two-tailed distribution, where (*) indicates statistical significance at ≤ 0.05.

Figure 6: Quercetin loaded tragacanth polymer coated zinc copper bimetallic nanoparticles reveal significant amoebistatic properties against *A. castellanii*. QUE-TRG-ZnCuNPs and Quercetin alone (100 µg per mL) demonstrated significant amoebistatic activity. The data is representative of at least 3 independent experiments, performed in duplicate and are presented as the mean ± standard error. Additionally, P-values were

View Article Online
DOI: 10.1039/D5PM00201J

calculated using a two-sample t-test with a two-tailed distribution, where (*) indicates statistical significance at $P \leq 0.05$.

Figure 7: Quercetin loaded tragacanth polymer coated zinc copper bimetallic nanoparticles significantly reduced encystment of *A. castellanii.*

QUE-TRG-ZnCuNPs and Quercetin alone (100 µg per mL) exhibited significant effects on encystation. The data is representative of at least 3 independent experiments, performed in duplicate and are presented as the mean ± standard error. Additionally, P-values were calculated using a two-sample t-test with a two-tailed distribution, where (*) indicates statistical significance at $P \leq 0.05$.

Figure 8: Quercetin loaded tragacanth polymer coated zinc copper bimetallic nanoparticles reveal significant effects on the excystment of *A. castellanii*. QUE-TRG-ZnCuNPs and Quercetin alone (100 µg per mL) exhibited significant effects on excystation. The data is representative of several independent experiments, performed in duplicate and are presented as the mean ± standard error. Additionally, P-values were calculated using a two-sample t-test with a two-tailed distribution, where (*) indicates statistical significance at $P \leq 0.05$.

Figure 9: Quercetin loaded tragacanth polymer coated zinc copper bimetallic nanoparticles exhibited decrease in amoeba-mediated cytotoxicity against human cells. At 100 µg per mL, QUE-TRG-ZnCuNPs significantly reduced amoebae-driven human cell cytopathogenicity. The data is representative of several independent experiments, performed in duplicate and are presented as the mean ± standard error. Additionally, P-values were calculated using a two-sample t-test with a two-tailed distribution, where (*) indicates statistical significance at $P \leq 0.05$.

View Article Online
DOI: 10.1039/D5PM00201J

Table 1: Characterization of TRG-ZnCuNPs and QUE-TRG-ZnCuNPs for size, PDI, zeta-potential, and %DEE.

S no.	***Samples***	***Size (nm)***	***PDI***	***Zeta potential (mV)***	***%DEE***
1.	TRG-ZnCuNPs	194.7 ± 11.3	0.257 ± 0.031	-25.5 ± 1.65	---
2.	QUE-TRG-ZnCuNPs	286.1 ± 2.9	0.183 ± 0.092	-30.4 ± 3.54	58.6 ± 2.85

View Article Online
DOI: 10.1039/D5PM00201J

Fig. 1

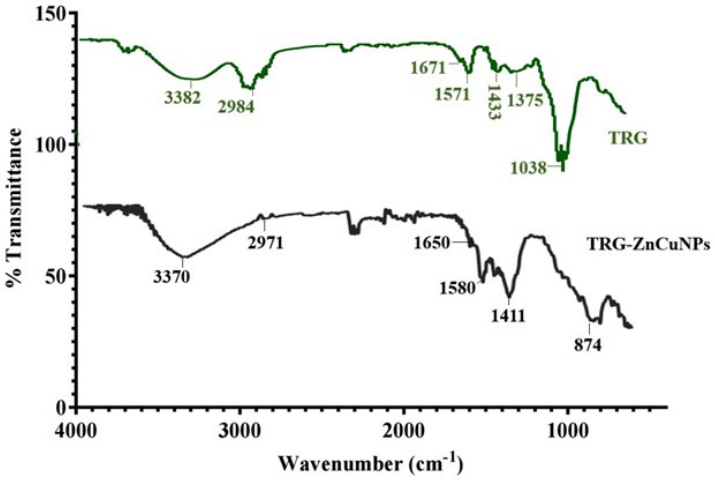

190x275mm (96 x 96 DPI)

View Article Online
DOI: 10.1039/D5PM00201J

Fig. 2

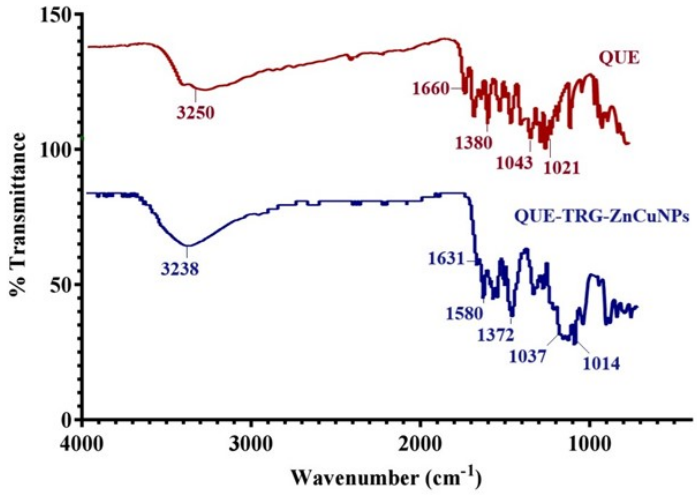

190x275mm (96 x 96 DPI)

View Article Online
DOI: 10.1039/D5PM00201J

Fig. 3

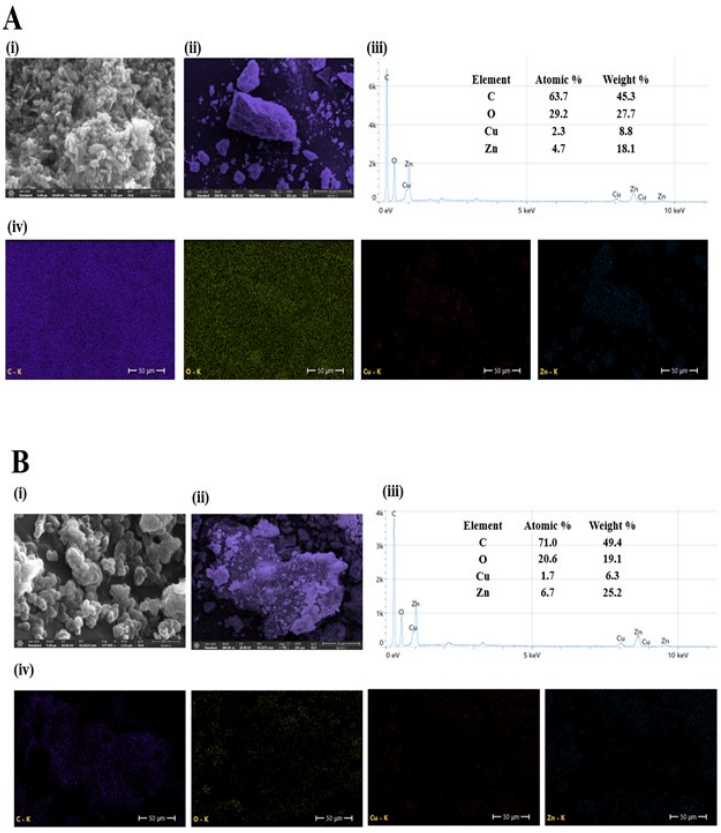

190x275mm (96 x 96 DPI)

View Article Online
DOI: 10.1039/D5PM00201J

Fig. 4

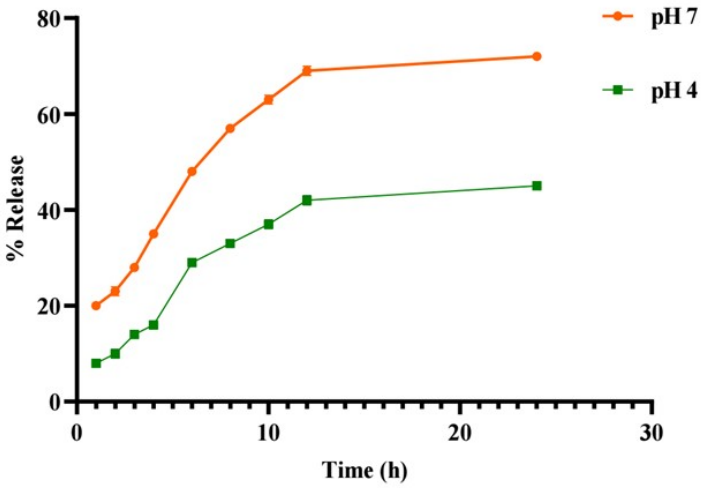

190x275mm (96 x 96 DPI)

View Article Online
DOI: 10.1039/D5PM00201J

Fig. 5

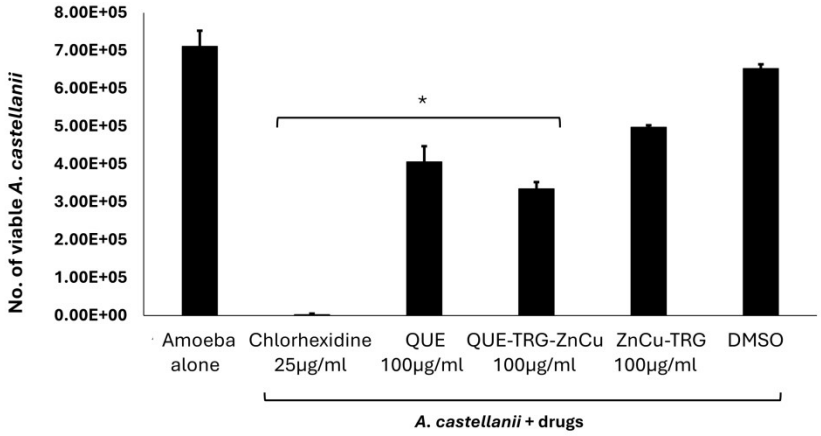

275x190mm (300 x 300 DPI)

View Article Online
DOI: 10.1039/D5PM00201J

Fig. 6

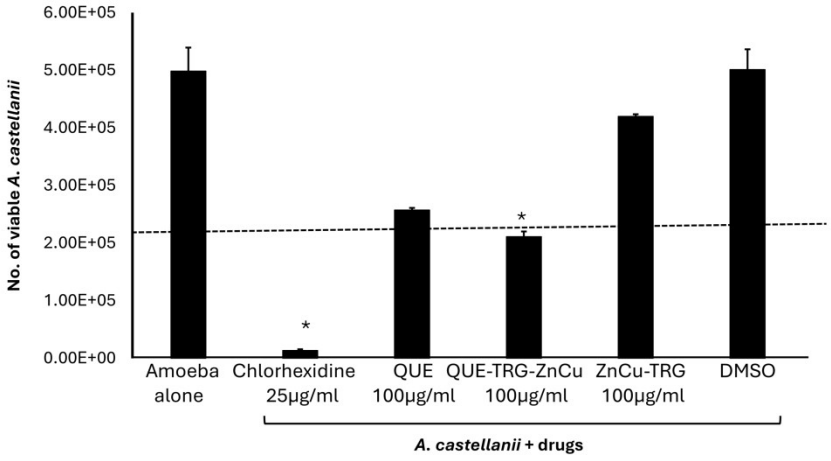

275x190mm (300 x 300 DPI)

View Article Online
DOI: 10.1039/D5PM00201J

Fig. 7

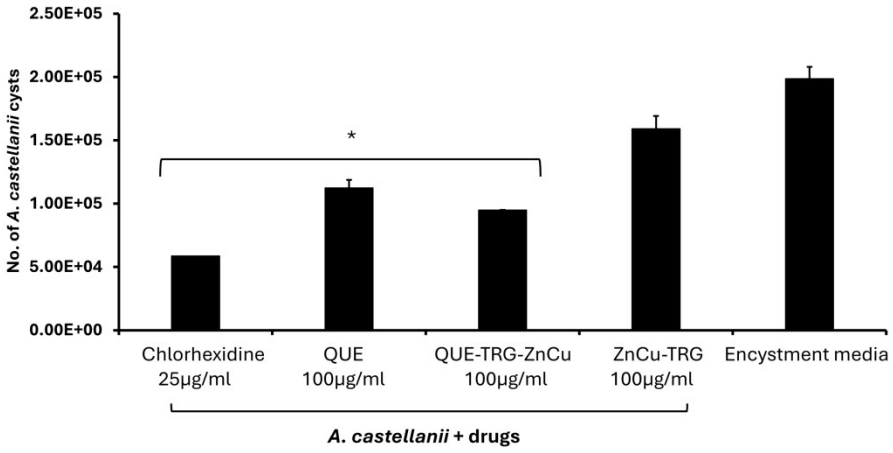

275x190mm (300 x 300 DPI)

View Article Online
DOI: 10.1039/D5PM00201J

Fig. 8

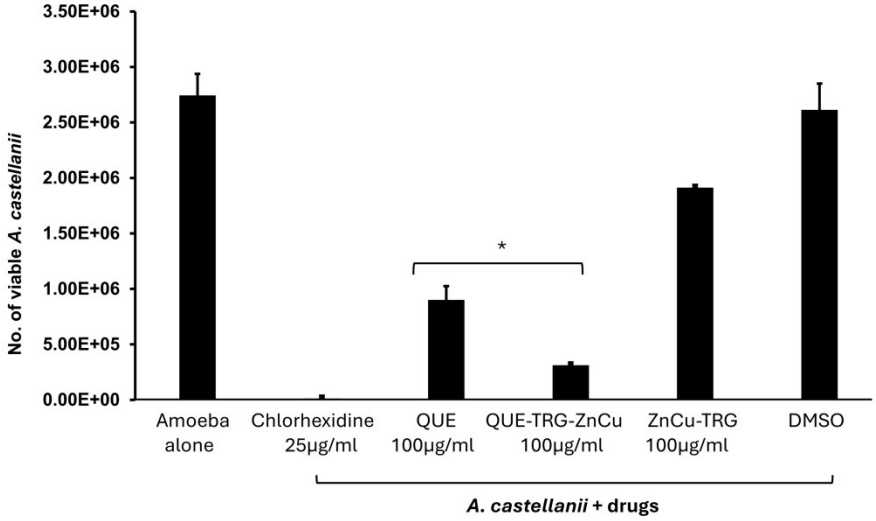

275x190mm (300 x 300 DPI)

View Article Online
DOI: 10.1039/D5PM00201J

Fig. 9

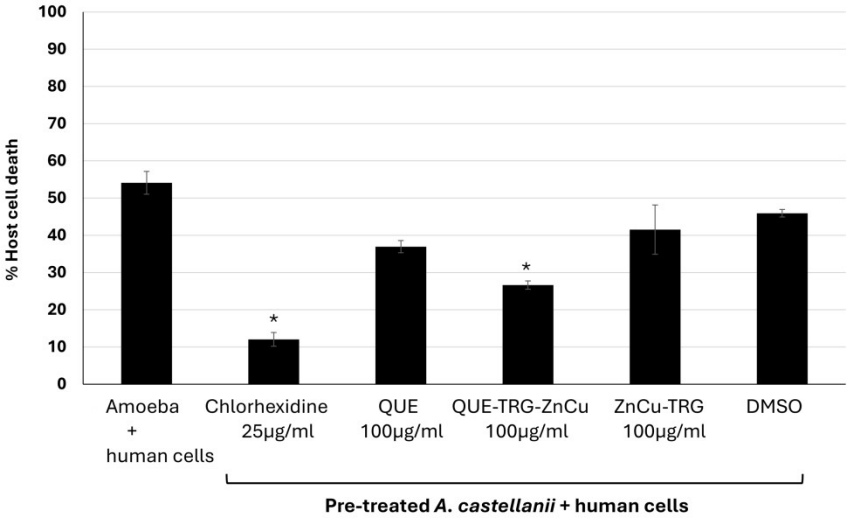

275x190mm (300 x 300 DPI)

DOI: 10.1039/D5PM00201J

Data availability statement: The data supporting this article have been included in the manuscript.